ascribed satisfactorily to environmental changes of β37-Trp and α42-Tyr. Since simple changes in dielectric field might induce intensity changes of Raman bands but not a noticeable frequency shift, we infer that changes of β37-Trp should involve a change of the hydrogen bonding at the NH group so that it could exhibit an appreciable frequency shift. Since β37-Trp (C2) is in contact with the α subunit at the FG corner, it is highly likely that the movement of proximal His (F8) upon ligation or deligation of the sixth ligand (O_2 or CO) is conveyed to the subunit surface through the F helix.

The 1604-cm^{-1} band in Figure 3 is associated with the split ν_8 band of benzene ring of Tyr and Phe. In the 218-nm excited RR spectra of amino acid solutions containing a known amount of perchlorate ions (used as an internal intensity standard), which were obtained in the same instrumental conditions as the present experiments (not shown), the intensity ratio of the 1613-cm^{-1} band to the 1557-cm^{-1} band of Trp was 0.3, and the intensity of the ν_{8a} band of Tyr was greater than that of the 1557-cm^{-1} band by a factor of 5. Therefore, the intensity contribution of Trp residues to the shoulder at 1613 cm^{-1} would not be large. This shoulder would rather arise from the high-frequency counterpart of the split ν_8 band of Tyr (ν_{8a}). However, it should be noted that the intensities of the ν_8 bands of Phe and Tyr were alike in the 218-nm excited RR spectra of amino acid solutions with an intensity standard, and the number of Phe residues is more than twice as large as Tyr residues for Hb A. Accordingly, the major part of intensity of the 1604-cm^{-1} band in Figure 3 would arise from Phe residues.

The 1011-cm^{-1} band of Trp arises from the breathing-like vibration of the benzene ring.[37] The intensity reduction of this band and other Trp bands may imply a decrease in the absorbance at 218 nm and thus a stacking of the Trp with other aromatic residues. Such stacking would also interpret the intensity reduction of the 1613-cm^{-1} shoulder if the band were due to the Trp contribution. Alternatively, if the shoulder were due to the Tyr contribution, it would be attributed to α42-Tyr as explained by Su et al.[30] Further investigation with a mutant Hb is desirable.

For either assignment, it became evident that environmental changes of the aromatic residues at the α_1–β_2 interface occurred at 10–20 μs after the photolysis. This is consistent with the results from kinetic absorption studies,[12,14] which pointed out that the quaternary structure changes around 20 μs after the photolysis of COHb. However, there are evidences for faster changes of the structure. A deoxyHb-like visible absorption spectrum is generated with a time constant of 0.35 ps.[15a] Hofrichter et al.[14] pointed out from a transient absorption study the presence of two other relaxations with time constants of 100 and 800 ns. The RR ν_{Fe-His} frequency relaxes in the time range from 10 ns to 1 μs,[20b,c] but the porphyrin skeletal stretching frequencies associated with the core size of porphyrin (ν_{10}, ν_{11}, and ν_{19}) relax in the time range between 20 and 300 ns.[19b,c] In the present measurements, data are lacking in the time range between Δt_d = 10 ns and 5 μs, where some other delay technique would be required, but it should be emphasized the amount of the changes occurring during this period is one-third of that occurring between 10 and 20 μs. Due to rebinding of CO to the photodissociated species, the complete curve describing the behavior after photolysis could not be derived from the present experiments. In addition, there are a few other small spectral changes that may reflect structural changes different from those discussed here, but their poor signal-to-noise ratio did not allow us to discuss them at the present stage. A more detailed study with the improved sample chamber is in progress.

In conclusion, the present observations strongly suggest that the ligand dissociation from the heme iron is communicated to the F helix through the Fe–His bond, and the movement of the F helix causes a change in the α_1–β_2 contact. It is unlikely that the dissociated CO triggers the quaternary structure change through the interaction with the distal His (E7).

Acknowledgment. We express our gratitude to Prof. Hideki Morimoto of Osaka University for stimulating discussion and to Dr. John Hougen of National Bureau of Standards for reading the manuscript.

Registry No. Inositol hexaphosphate, 83-86-3.

(39) (a) Perutz, M. F.; Ladner, J. E.; Simon, S. R.; Ho, C. *Biochemistry* **1974**, *13*, 2163–2173. (b) Perutz, M. F.; Fersht, A. R.; Simon, S. R.; Roberts, C. K. *Biochemistry* **1974**, *13*, 2174–2185.

Unequivocal Proof of Slowed Chromium Tricarbonyl Rotation in a Sterically Crowded Arene Complex: An X-ray Crystallographic and Variable-Temperature High-Field NMR Study of $(C_6Et_5COCH_3)Cr(CO)_3$

Patricia A. Downton, Bavani Mailvaganam, Christopher S. Frampton, Brian G. Sayer, and Michael J. McGlinchey*

Contribution from the Department of Chemistry, McMaster University, 1280 Main Street West, Hamilton, Ontario, Canada L8S 4M1. *Received March 20, 1989*

Abstract: The low-temperature ^{13}C NMR spectrum of $(C_6Et_5COCH_3)Cr(CO)_3$ is explicable only in terms of a single stereoisomer, i.e., the 1-proximal-acetyl-2,4,6-distal-3,5-proximal conformer. The $Cr(CO)_3$ resonance is split 2:1 both in solution at −100 °C and in the CPMAS solid-state spectrum at 30 °C; these data demonstrate that $Cr(CO)_3$ rotation has stopped on the NMR time scale. Crystals of $(C_6Et_5COCH_3)Cr(CO)_3$ are triclinic, of space group $P\bar{1}$ with a = 8.876 (2) Å, b = 9.458 (3) Å, c = 13.383 (4) Å, α = 95.26 (2)°, β = 98.89 (2)°, γ = 111.54 (2)°, V = 1018.9 (5) Å^3, D_c = 1.29 g cm^{-3}, D_m = 1.28 g cm^{-3} for Z = 2, and R_1 = 0.0659 (R_2 = 0.0753) for 2673 unique reflections (R_1 = 0.0501, R_2 = 0.0547 for 2198 reflections with $I > 2.5\sigma(I)$). The alternating proximal–distal arrangement of substituents is in accord with the NMR data. These results are discussed in the context of previous reports on $(C_6Et_6)Cr(CO)_2L$ complexes.

The dynamic behavior of tricarbonyl(η^6-hexaethylbenzene)-chromium, **1**, in solution has been the subject of some debate over a period of several years. In 1979 we reported the solid-state ^{13}C NMR spectrum of **1** and noted that the methyl, methylene, and ring carbon resonances were not single peaks but instead appeared as pairs of equally intense lines.[1] This observation was interpreted

0002-7863/90/1512-27$02.50/0

in terms of a 1,3,5-distal-2,4,6-proximal conformation (I) for the C_6Et_6 ligand since such a structure would split the 6-fold degeneracy of the arene; the hexaethylbenzene (HEB) moiety would thus have local D_{3d} symmetry and the complex overall would be C_{3v}.

A subsequent X-ray crystallographic investigation by Hunter et al. revealed that our proposal was indeed correct. Furthermore, these authors established that the same conformation is also adopted in solution;[2] at room temperature, the methyl, methylene, and arene ring carbons appear as singlets, but at low temperature, these resonances are again split, as in the solid state. Moreover, these authors claimed that one could use variable-temperature T_1 measurements to evaluate the barrier to rotation of the $Cr(CO)_3$ group and reported that it is unlikely to exceed $\approx$5 kcal mol^{-1}. (They admitted, however, that it was not possible to separate the contributions from tripodal rotation and overall molecular tumbling.) Although it is undoubtedly true that there is no electronic barrier to rotation[3] and that in $(C_6H_6)Cr(CO)_3$ the tripod behaves as an unhindered rotor, we were somewhat skeptical of the claim of free rotation in $(HEB)Cr(CO)_3$, **1**.[4] The X-ray crystallographic data would suggest that considerable steric hindrance would be encountered by a carbonyl in its attempts to manoeuver its way past a proximal methyl group. In fact, the problem cannot be solved unequivocally for $(HEB)Cr(CO)_3$ itself since the molecular point group remains effectively C_{3v} whether the tripod spins or not. Therefore, we chose to break the 3-fold symmetry of the molecule by incorporating a thiocarbonyl ligand into the tripod.

The X-ray crystal structure of $(HEB)Cr(CO)_2CS$, **2**, closely resembles that of the tricarbonyl analogue, **1**, but the low-temperature ^{13}C NMR spectrum of **2** exhibits for the methyl, methylene, and arene ring carbons a 2:1:2:1 pattern in each case.[5] Clearly, the molecule must now have overall C_s symmetry, and we took this as evidence for the cessation of tripodal rotation on the NMR time scale. This claim was challenged by Hunter and Mislow, who agreed that **2** must possess mirror symmetry but pointed out that this could be achieved merely by letting the HEB itself adopt a C_s conformation, as in the 1,2,3,5-distal-4,6-proximal conformation (II).[6] Such an arrangement for the ethyl groups has been observed previously in the salt $[(HEB)Fe(C_5H_5)]^+[PF_6]^-$, **3**,[7] and also in $(HEB)Cr(CO)_2PMe_3$, **4**.[8] If the thiocarbonyl complex **2** were to adopt conformation II in solution, it would bestow C_s symmetry on the system and one could explain the 2:1:2:1 patterns in the ^{13}C NMR spectrum without the need to invoke slowed tripodal rotation.

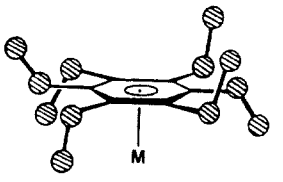

(I)

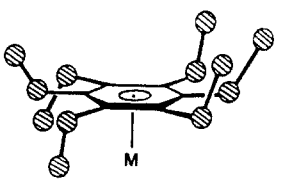

(II)

1: M = $Cr(CO)_3$

2: M = $Cr(CO)_2CS$

3: M = $CpFe^+$

4: M = $Cr(CO)_2PMe_3$

5: M = $Cr(CO)_2NO^+$

It was thus incumbent upon us to show that the HEB conformations adopted by molecule **2** were the same both in the solid state and in solution. At this point we reported[9] that the solid-state ^{13}C NMR spectrum of **2** closely resembled the solution spectrum at low temperature, suggesting that the same molecular conformation was extant in both phases. Furthermore, a comparison of the NMR spectra of all of the structurally characterized HEB–metal complexes revealed that methyl carbons positioned distal with respect to the organometallic moiety resonate at $\delta \approx 14$, whereas proximal methyls in Cr complexes are found in the range δ 18–20. Likewise, chemical shift ranges for methylene carbons and ring carbons are also readily assignable. We therefore felt confident that our claim for slowed tripodal rotation was on firm ground. Although Hunter and Mislow have reiterated[10] their view that the case is still "not proven", we have recently reinforced our position with the observation that the nitrosyl complex $[(HEB)Cr(CO)_2NO]^+BF_4^-$, **5**, also possesses the 1,3,5-distal-2,4,6-proximal conformation in the solid state and, like **2**, exhibits 2:1:2:1 ^{13}C NMR patterns for the methyl, methylene, and arene ring carbon environments.[11]

Although we felt the accumulated weight of evidence to be strongly supportive of our position, the ingenious arguments of Hunter and Mislow had been persuasively and eloquently stated, so we chose to attack the problem in a different fashion. To this end, we prepared the tricarbonylchromium complex of pentaethylacetophenone and now report X-ray crystallographic and variable-temperature NMR spectroscopic data on this molecule.

Results and Discussion

Our previous attempts to provide unequivocal evidence of slowed rotation of the organometallic fragment in complexes of the type $(HEB)Cr(CO)_2L$ were based on the idea of breaking the 3-fold degeneracy of the tripod and then detecting this lowered symmetry via the NMR behavior of the HEB ligand. An alternative approach would be to synthesize an arene that itself has only mirror symmetry but that can present a conformation closely analogous to the 1,3,5-distal-2,4,6-proximal arrangement found in **1**, **2**, and **5**. In principle, the cessation of tripodal rotation would then be reflected in a splitting of the 3-fold symmetry of the $Cr(CO)_3$ moiety.

The reaction of $CH_3COCl/AlCl_3$ with hexamethylbenzene to give pentamethylacetophenone occurs in very poor yield even upon prolonged heating at 85 °C.[12] In contrast, the corresponding reaction with hexaethylbenzene in CS_2 at 45 °C is an exceedingly facile process which gives pentaethylacetophenone, **6**, in 80% yield. Presumably, the driving force for the reaction is the loss of ethylene from the intermediate cationic species. Treatment of **6** with $Cr(CO)_6$ via the standard protocol yields $(C_6Et_5COCH_3)Cr(CO)_3$,

(1) Maricq, M. M.; Waugh, J. S.; Fletcher, J. L.; McGlinchey, M. J. *J. Am. Chem. Soc.* **1978**, *100*, 6902.

(2) (a) Hunter, G.; Iverson, D. J.; Mislow, K.; Blount, J. F. *J. Am. Chem. Soc.* **1980**, *102*, 5942. (b) Iverson, D. J.; Hunter, G.; Blount, J. F.; Damewood, J. R., Jr.; Mislow, K. *J. Am. Chem. Soc.* **1981**, *103*, 6073.

(3) Albright, T. A.; Hofmann, P.; Hoffmann, R. *J. Am. Chem. Soc.* **1977**, *99*, 7546.

(4) Attempts to slow the rotation of a $Cr(CO)_3$ group on the NMR time scale have been the subject of many elegant investigations: (a) Nambu, M.; Siegel, J. S. *J. Am. Chem. Soc.* **1988**, *110*, 3675. (b) Acampora, A.; Ceccon, A.; Dal Farra, M.; Giacometti, G.; Rigatti, G. *J. Chem. Soc., Perkin Trans. 2* **1977**, 483. (c) Delise, P.; Allegra, G.; Mognaschi, E. R.; Chierico, A. *J. Chem. Soc., Faraday Trans. 2* **1975**, 207. (d) Jula, T. F.; Seyferth, D. *Inorg. Chem.* **1968**, *7*, 1245. (e) Emanuel, R. V.; Randall, E. W. *J. Chem. Soc. A* **1969**, 3002. (f) Barbieri, G.; Taddei, F. *Chem. Commun.* **1970**, 312. (g) Jackson, W. R.; Jennings, W. B.; Spratt, R. *Chem. Commun.* **1970**, 593. (h) Segard, C.; Roques, B. P.; Pommier, C.; Guiochon, G. *Anal. Chem.* **1971**, *43*, 1146. (i) Bennett, M. A.; Robertson, G. B.; Smith, A. K. *J. Organometal. Chem.* **1972**, *43*, C41. (j) Randall, E. W.; Rosenberg, E.; Milone, L. *J. Chem. Soc., Dalton Trans.* **1973**, 1692. (k) Roques, B. P.; Segard, C.; Combrisson, S.; Wehrli, F. *J. Organometal. Chem.* **1974**, *73*, 327. (l) Bodner, G. M.; Todd, L. J. *Inorg. Chem.* **1974**, *13*, 360. (m) van Meurs, F.; van der Toorn, J. M.; van Bekkum, H. *J. Organometal. Chem.* **1976**, *113*, 341. (n) Jackson, W. R.; Pincombe, C. F.; Rae, I. D.; Rash, D.; Wilkinson, B. *Aust. J. Chem.* **1976**, *29*, 2431.

(5) McGlinchey, M. J.; Fletcher, J. L.; Sayer, B. G.; Bougeard, P.; Faggiani, R.; Lock, C. J. L.; Bain, A. D.; Rodger, C. A.; Kuendig, E. P.; Astruc, D.; Hamon, J.-P.; LeMaux, P.; Top, S.; Jaouen, G. *J. Chem. Soc., Chem. Commun.* **1983**, 634.

(6) Hunter, G.; Mislow, K. *J. Chem. Soc., Chem. Commun.* **1984**, 172.

(7) Hamon, J. R.; Saillard, J.-Y.; LeBeuze, A.; Astruc, D.; McGlinchey, M. J. *J. Am. Chem. Soc.* **1982**, *104*, 7549.

(8) Blount, J. F.; Hunter, G.; Mislow, K. *J. Chem. Soc., Chem. Commun.* **1984**, 170.

(9) McGlinchey, M. J.; Bougeard, P.; Sayer, B. G.; Hofer, R.; Lock, C. J. L. *J. Chem. Soc., Chem. Commun.* **1984**, 789.

(10) Hunter, G.; Weakley, J. R.; Mislow, K.; Wong, M. G. *J. Chem. Soc., Dalton Trans.* **1986**, 577.

(11) Mailvaganam, B.; Frampton, C. S.; Sayer, B. G.; McGlinchey, M. J. *Organometallics*, submitted for publication.

(12) Hopff, H.; Wick, A. K. *Helv. Chim. Acta* **1960**, *43*, 1473.

Table I. ^{13}C NMR Data for Hexaethylbenzene, Pentaethylacetophenone, and Their $Cr(CO)_3$ Complexes, **1** and **7**

		HEB[a]	PEAP[a]	(HEB)Cr(CO)$_3$[b]	(PEAP)Cr(CO)$_3$	
	CH_3		33.57		36.93[c]	35.9[d]
1-acetyl	C=O		209.27		205.01	205.4
	C(Ar)		142.19		106.65	107.0
	CH_3	15.5	16.59	14.2	15.25	15.3
2,6-diethyl	CH_2	21.6	23.97	22.8	23.99	26.6/25.8
	C(Ar)	137.2	134.35	117.2	113.66	113.7/112.7
	CH_3	15.5	16.10	20.1	20.78	20.8
3,5-diethyl	CH_2	21.6	21.94	19.4	19.29	20.9
	C(Ar)	137.2	138.89	108.8	109.1	109.0/107.3
	CH_3	15.5	16.04	14.2	14.68	15.3
4-ethyl	CH_2	21.6	22.42	22.8	22.96	23.4
	C(Ar)	137.2	141.36	117.2	118.62	117.5
	$Cr(CO)_3$			235.4	235.0 [2]	233.4 [2]
					234.6 [1]	230.7 [1]

[a] HEB = hexaethylbenzene; PEAP = pentaethylacetophenone. [b] In this table, the proximal ethyls in (HEB)Cr(CO)$_3$ are C(1), C(3), and C(5); substituents at C(2), C(4), and C(6) are distal. Data obtained in CD_2Cl_2 at −71 °C [from ref 2]. [c] Data obtained in CD_2Cl_2 at −100 °C. [d] CPMAS data at +30 °C.

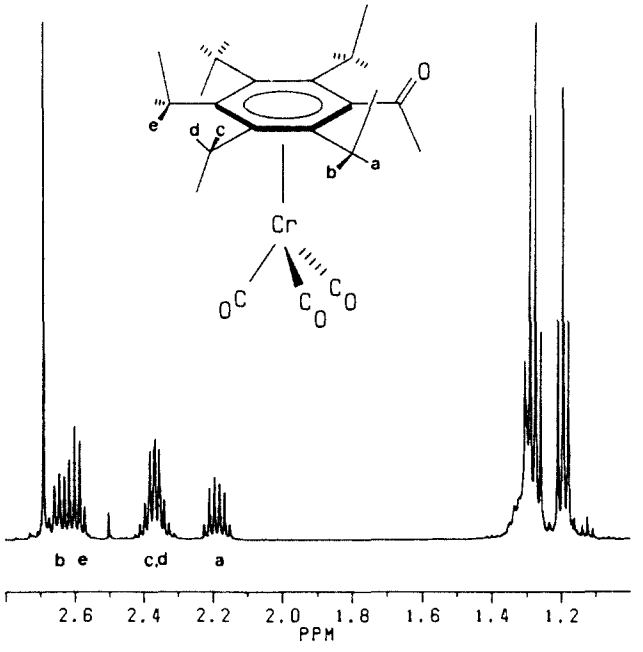

Figure 1. 500-MHz ^1H NMR spectrum of $(C_6Et_5COCH_3)Cr(CO)_3$, **7**, in CD_2Cl_2.

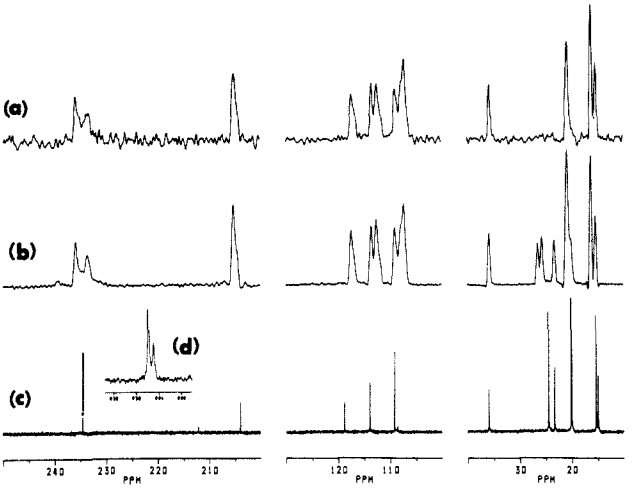

Figure 2. ^{13}C NMR spectra of $(C_6Et_5COCH_3)Cr(CO)_3$, **7**. (a) Dipolar dephased 25.1-MHz CPMAS solid-state spectrum in which the methylene resonances have been suppressed. (b) Normal 25.1-MHz CPMAS solid-state spectrum, recorded at +30 °C. (c) 125.7-MHz high-resolution spectrum in CD_2Cl_2 at +30 °C. (d) Metal carbonyl resonances at −100 °C.

7, which was recrystallized from CH_2Cl_2/heptane to yield yellow parallelepiped crystals suitable for X-ray diffraction studies.

High-Resolution ^{13}C and ^1H NMR Spectroscopies. Not surprisingly, the ^{13}C NMR spectrum of pentaethylacetophenone, **6**, is in many ways reminiscent of hexaethylbenzene. Of course, the molecule has effective C_{2v} symmetry since rotation of the acetyl and ethyl groups should be fast on the NMR time scale at room temperature. An interesting observation is the resonance position of the carbonyl carbon in **6** which is found at δ 209 as opposed to the shift of δ 196 in acetophenone itself. Such effects have been reported previously, and indeed one can correlate the deshielding of the ketonic carbon with the steric bulk of the ortho substituents that inhibit coplanarity of the carbonyl group and the phenyl ring.[13] Moreover, we have carried out molecular mechanics calculations on HEB and on pentaethylacetophenone. As anticipated from earlier data,[2] the most stable conformer in each case is the one in which the methyl substituents are oriented alternately above and below the plane of the arene ring. In the former, one calculates a C(arene)—CH_2—CH_3 angle of 112° which is in reasonable accord with the X-ray crystallographically determined value for HEB of 112.8°;[2] in the latter, the results suggest that the C(arene)—CH_2—CH_3 angles would remain almost unchanged but that the C(arene)—C(=O)—CH_3 angle would be ≈117°. Such an angle would be similar to that observed in **1**, where the proximal ethyls have opened up to 115.8°.[2] It thus appears that pentaethylacetophenone has the potential to mimic HEB and so make a comparison of their $Cr(CO)_3$ complexes a worthwhile undertaking.

The ^{13}C and ^1H NMR spectra of $(C_6Et_5COCH_3)Cr(CO)_3$, **7**, are particularly informative. First of all, they remain essentially unchanged over the temperature range +30 to −100 °C except for one feature, which we shall discuss presently. Not only is it clear that every peak is readily assignable to a single conformer but one can also show that this stereoisomer is the 1-proximal-acetyl-2,4,6-distal-3,5-proximal-pentaethyl complex, as in Figure 1, which also shows the ^1H NMR spectrum of **7**. (We here define a proximal acetyl as possessing a proximal methyl group.) The solid-state and solution NMR spectra of **7** appear in Figure 2.

As outlined above, we can assign ^{13}C methyls resonating at approximately δ 20 as being proximal and those at δ ≈14 to a distal environment. The ethyl group of single relative intensity (i.e., the 4-ethyl substituent) is thus clearly distal; it shows CH_3, CH_2, and ring carbon resonances at δ 14.68, 22.96, and 118.62 which, as shown in Table I, correspond extremely well with the distal chemical shifts in **1**. Similarly, the doubly intense ethyl resonances at δ 20.78, 19.29, and 109.10 are unambiguously classifiable as the methyl, methylene, and ring carbons of the proximal ethyl substituents at the 3,5-positions. Finally, the remaining doubly intense peaks are assignable to the distal ethyls at the 2,6-positions. The connectivity of the methyl and methylene carbon pairs was trivial to establish via the ^1H–^{13}C shift-correlated and ^1H–^1H

(13) Stothers, J. B.; Lauterbur, P. C. *Can. J. Chem.* **1964**, *42*, 1563.

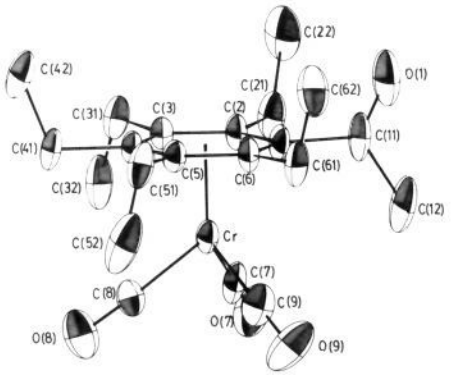

Figure 3. View of $(C_6Et_5COCH_3)Cr(CO)_3$, **7**, showing atom numbering scheme. The labels for arene carbons C(1) and C(4) have been omitted for clarity.

COSY two-dimensional experiments. The proton chemical shifts (see Figure 1) are also in complete accord with these assignments. Thus, the methylene pairs proximate to the acetyl substituent have a large chemical shift difference. The protons designated H_A lie in the shielding cone of the ketonic carbonyl and are markedly shifted from their H_B partners which have chemical shifts appropriate for methylene protons in a proximal ethyl group.[9,11] Of course, in the chromium complex **7**, there can be no interconversion of the H_A and H_B (or H_C and H_D) environments by ethyl and acetyl rotations as can happen in free $C_6Et_5COCH_3$. Even should rapid ethyl rotation occur (and presumably it does at room temperature), the methylene proton pairs at C(2)/C(6) and C(3)/C(5) are always magnetically nonequivalent.

The conclusion that can be drawn from the ^1H and ^{13}C NMR data is that in solution the only detectable conformer of **7** has the 2,4,6-distal-3,5-proximal arrangement of ethyl groups. Now, if the orientation of the 1-acetyl substituent is proximal, as in Figure 1, the $Cr(CO)_3$ finds itself in an environment that is remarkably similar to that already established for **1**. In this case, however, the tricarbonylchromium fragment would be attached to an arene possessing C_s rather than C_{3v} symmetry, so the differentiation between a rotating or nonrotating tripod is easily made. As shown in Figure 2, the ^{13}C signal at δ 234 attributable to the chromium carbonyl moiety is clearly split into a 2:1 pattern at −100 °C, thus showing that the $Cr(CO)_3$ moiety now has mirror symmetry and that the original 3-fold degeneracy has been broken.[14] The imposition of C_s symmetry on the $Cr(CO)_3$ unit has a simple rationale, and the conclusion is inescapable: *we have slowed the tripodal rotation on the NMR time scale in 7 and, by implication, in* $(HEB)Cr(CO)_3$.

Structure. The X-ray crystal structure of **7** was determined, and a view of the molecule with atom numbering scheme is depicted in Figure 3.

Even though one of the ethyl groups is replaced by an acetyl substituent, the stereochemistry of $(C_6Et_5COCH_3)Cr(CO)_3$ is remarkably similar to that of $(HEB)Cr(CO)_3$, $(HEB)Cr(CO)_2CS$, and $(HEB)Cr(CO)_2NO^+$, with the acetyl and ethyl groups adopting the 1-proximal-acetyl-3,5-proximal-2,4,6-distal-pentaethyl conformation. The disposition of the tripodal fragment is such as to place the carbonyl groups within a few degrees of being perfectly eclipsed with respect to the arene carbons that are bonded to the distal ethyl groups; the torsional angles for $C(2)–C_{trd}–Cr–C(7)$, $C(4)–C_{trd}–Cr–C(8)$ and $C(6)–C_{trd}–Cr–C(9)$ are 4.6°, 3.5°, and 3.1°, respectively. The average $C_{ar}–CH_2–CH_3$ bond angle for the three distal ethyl groups is 111.7° (111.9° in **1**) and the two proximal ethyl groups give a mean value of 116.4° (115.8° in **1**) while that of the proximal $C_{ar}–CO–CH_3$ is 119.4°. The ring centroid–chromium distance is 1.725 Å in **7** compared to 1.729 Å in **1**. The mean dihedral angles made between the least-squares plane of the arene ring and the distal and proximal $C_{ar}–CH_2–CH_3$ groups are 90.3° and 89.1°, while the mean bond angles at a distal or proximal carbon within the arene ring are 120.4° and 119.6°, respectively. A stereoscopic view of the unit cell contents is shown in Figure 4. The crystal packing appears to be determined by van der Waals forces only with the $Cr(CO)_3$ tripods stacked in an interlocking manner. No unusual inter-molecular contacts are observed.

Solid-State ^{13}C NMR Spectroscopy. In order to relate molecular structures in solution and in the solid state, it is frequently advantageous to compare the limiting low-temperature ^{13}C NMR spectrum in solution with the CPMAS data obtained on a solid sample.[15] However, one must recall that the NMR spectrum of the crystalline material reflects the contents of the unit cell rather than that of the point group of the individual molecule. Thus, the high-resolution ^{13}C spectrum of **7** obtained in dichloromethane solution exhibits a 1:2:2:1 pattern for the arene carbons in accord with the effective C_s point group of the molecule. In the solid state, however, there are two molecules of **7** per unit cell, and they are related merely by an inversion center. For example, the distal ethyl groups in the 2- and 6-positions of **7** are not required by symmetry to be magnetically equivalent; they may by coincidence have identical chemical shifts, but it is not mandatory. This point is beautifully made in the CPMAS ^{13}C NMR spectrum of $(C_6Et_5COCH_3)Cr(CO)_3$. As shown in Figure 2, the aromatic ring resonances of the C(2) and C(6) appear as a singlet (of intensity two) at δ 113.66 in the solution spectrum; in contrast, they give rise to two equally intense peaks at δ 113.7 and 112.7 in the solid-state NMR experiment. It is apparent that there is a very clear correlation between the solution and solid-state NMR spectra of **7**, thus indicating that the molecule adopts the same conformation in both phases. It is particularly noteworthy that the chromium carbonyl resonances are split in the CPMAS experiment just as they are at −100 °C in the high-resolution spectrum. There can be no doubt that (pentaethylacetophenone)tricarbonylchromium(0) adopts the 1-proximal–acetyl-2,4,6-distal-3,5-proximal-pentaethyl conformation in both the solid state and in solution and that there is cessation of tripodal rotation on the NMR time scale.

Conclusions

The remarkably similar structural and NMR spectroscopic parameters of $(C_6Et_5COCH_3)Cr(CO)_3$, **7**, of $(C_6Et_6)Cr(CO)_3$, **1**, of $(C_6Et_6)Cr(CO)_2CS$, **2**, and of $[(C_6Et_6)Cr(CO)_2NO]^+$, **5**, bear testimony to the fact that all four of these molecules adopt conformation I with alternating proximal and distal substituents both in the solid state and in solution and that tripodal rotation is slowed on the NMR time scale at low temperatures.

Experimental Section

All reactions were carried out under an atmosphere of dry nitrogen by employing conventional benchtop and glovebag techniques. All solvents were dried according to standard procedures before use. ^{13}C NMR and ^1H NMR spectra were recorded at 125.7 and 500 MHz, respectively, by using a Bruker AM500 spectrometer. Chemical shifts reported were referenced to tetramethylsilane. Solid-state ^{13}C spectra were obtained at 25.18 MHz on a Bruker MSL100 operating at 2.35 T. The CPMAS spectrum was obtained using a 1-ms contact time and a recycle time of 10 s. The dipolar dephased spectrum was obtained using a dephasing time of 50 μs, effectively eliminating signals from CH and CH_2 groups. Infrared spectra were recorded on a Perkin-Elmer 283 instrument using NaCl solution cells. Electron impact mass spectra were obtained on a VG Micromass 7070F with a source temperature of 200 °C and an accelerating voltage of 70 eV. Microanalytical data are from Guelph Chemical Laboratories, Guelph, Ontario.

$C_6Et_5COCH_3$ (6). Following the method of Hopff and Wick,[12] hexaethylbenzene (12.32 g, 50 mmol), acetyl chloride (4.00 g, 51 mmol), and anhydrous aluminum trichloride (7.35 g, 55 mmol) were heated under reflux in carbon disulfide for 4 h, during which time hydrogen chloride was evolved. The deep brown reaction mixture was treated with ice/HCl

(14) It is difficult to give a reliable estimate of the barrier to tripodal rotation since, even on an 11.7-T instrument, the ^{13}CO peak separation in solution is only 50 Hz and the coalescence phenomenon occurs over the temperature range 173–183 K. The Gutowsky–Holm approximation yields a barrier in the range 8.5–9.5 kcal mol^{-1}.

(15) Childs, R. F.; Varadarajan, A.; Lock, C. J. L.; Faggiani, R.; Fyfe, C. A.; Wasylishen, R. E. *J. Am. Chem. Soc.* **1982**, *104*, 2452.

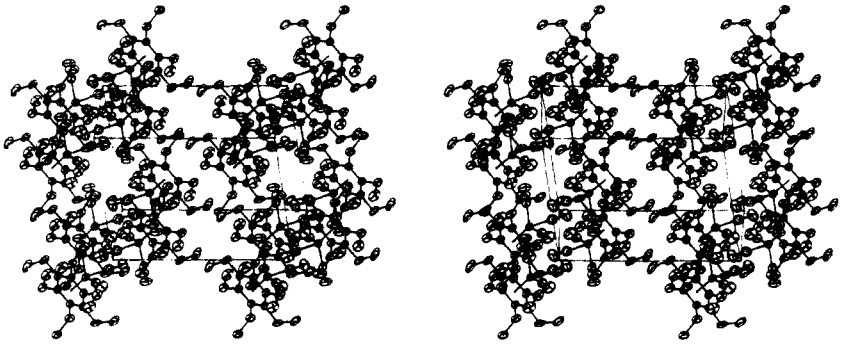

Figure 4. Stereoview of the unit cell, projection is [0 1 0].

Table II. Crystal Data for $(C_6Et_5COCH_3)Cr(CO)_3$, **7**

formula	$C_{21}H_{28}O_4Cr$
fw	396.44
system	triclinic
space group	$P\bar{1}$ no. 2
a, Å	8.876 (2)
b, Å	9.458 (3)
c, Å	13.383 (4)
α, deg	95.26 (2)
β, deg	98.89 (2)
γ, deg	111.54 (2)
V, Å^3	1018.9 (5)
Z	2
D_c (D_m), g cm^{-3}	1.29 (1.28)
$F(000)$	420.72 (420)
μ(Mo Kα), cm^{-1}	6.08 (5.34)
final R_1, R_2[a,d]	0.0659, 0.0753
weighting scheme	$w = (\sigma^2F + 0.0039F^2)^{-1}$
error in observation of unit weight[b]	1.3150
highest peak, e Å^{-3}; location	0.49; 0.125, 0.224, 0.117[c]
lowest peak, e Å^{-3}	−0.56

[a] $R_1 = \sum||F_o| - |F_c||/\sum|F_o|$; $R_2 = (\sum w(|F_o| - |F_c|)^2/\sum wF_o^2)^{1/2}$. [b] $S = (\sum w(|F_o| - |F_c|)^2/(m-n))^{1/2}$; m = number of reflections, n = number of variables. [c] 1.17 Å from Cr. [d] R_1 and R_2 for 2198 reflections with $I > 2.5\sigma(I)$ are 0.0501 and 0.0547, respectively.

Table III. Positional Parameters (×10^4) and U_{eq} (Å^2 × 10^4) for $(C_6Et_5COCH_3)Cr(CO)_3$, **7**, with Standard Errors in Parentheses

atom	x	y	z	U_{eq},[a] Å^2
Cr	2299.1 (8)	2305.2 (7)	1844.0 (5)	270
C(1)	3252 (5)	4563 (5)	2856 (3)	298
C(11)	2680 (6)	5904 (6)	2865 (4)	395
C(12)	1213 (8)	5789 (6)	2076 (6)	655
O(1)	3441 (6)	7030 (4)	3514 (3)	631
C(2)	2634 (5)	3406 (5)	3447 (3)	291
C(21)	1390 (6)	3519 (6)	4091 (4)	393
C(22)	2271 (9)	4456 (6)	5161 (4)	591
C(3)	3235 (5)	2201 (5)	3486 (3)	282
C(31)	2621 (6)	1007 (5)	4182 (4)	370
C(32)	1017 (6)	−386 (6)	3720 (5)	522
C(4)	4415 (5)	2167 (5)	2904 (3)	266
C(41)	5055 (6)	864 (5)	2931 (4)	357
C(42)	6557 (6)	1260 (6)	3809 (4)	445
C(5)	5080 (5)	3352 (5)	2316 (3)	278
C(51)	6455 (5)	3370 (6)	1752 (4)	377
C(52)	5906 (8)	2486 (8)	657 (4)	567
C(6)	4477 (5)	4550 (5)	2288 (3)	294
C(61)	5153 (6)	5845 (5)	1683 (4)	421
C(62)	6656 (8)	7197 (6)	2324 (5)	584
C(7)	66 (6)	1537 (5)	1787 (3)	359
O(7)	−1358 (4)	1040 (5)	1763 (3)	567
C(8)	2011 (6)	410 (6)	1169 (4)	394
O(8)	1874 (6)	−785 (5)	783 (4)	724
C(9)	1928 (6)	2919 (6)	588 (4)	482
O(9)	1743 (6)	3343 (6)	−193 (3)	740

[a] $U_{eq} = {}^1/_3(U_{11} + U_{22} + U_{33} + 2U_{23}\cos\alpha + 2U_{13}\cos\beta + 2U_{12}\cos\gamma)$.

and extracted with ether. Removal of the solvent and recrystallization from CH_2Cl_2/hexane gave white needles of pentaethylacetophenone, **6** (10.4 g, 40 mmol; 80%), mp 136–137 °C.

Table IV. Selected Bond Lengths (Å) and Bond Angles (deg) for $(C_6Et_5COCH_3)Cr(CO)_3$, **7**, with Estimated Standard Deviations in Parentheses

	Chromium Coordination		
Cr–C(1)	2.213 (4)	Cr–C(7)	1.830 (5)
Cr–C(2)	2.223 (4)	Cr–C(8)	1.842 (5)
Cr–C(3)	2.250 (4)	Cr–C(9)	1.849 (6)
Cr–C(4)	2.224 (4)	C(7)–O(7)	1.169 (6)
Cr–C(5)	2.255 (4)	C(8)–O(8)	1.154 (6)
Cr–C(6)	2.236 (4)	C(9)–O(9)	1.163 (7)
Cr–C_{trd}	1.725 (2)		
Cr–C(7)–O(7)	179.1 (4)	C_{trd}–Cr–C(7)	127.45
Cr–C(8)–O(8)	177.0 (5)	C_{trd}–Cr–C(8)	125.89
Cr–C(9)–O(9)	177.8 (6)	C_{trd}–Cr–C(9)	125.74
	Pentaethylacetophenone		
C(1)–C(2)	1.406 (6)	C(4)–C(41)	1.536 (6)
C(2)–C(3)	1.426 (6)	C(5)–C(51)	1.527 (6)
C(3)–C(4)	1.407 (6)	C(6)–C(61)	1.520 (6)
C(4)–C(5)	1.429 (6)	C(11)–O(1)	1.211 (6)
C(5)–C(6)	1.421 (6)	C(11)–C(12)	1.507 (8)
C(6)–C(1)	1.422 (6)	C(21)–C(22)	1.536 (8)
C(1)–C(11)	1.529 (6)	C(31)–C(32)	1.532 (7)
C(2)–C(21)	1.529 (6)	C(41)–C(42)	1.538 (7)
C(3)–C(31)	1.529 (6)	C(51)–C(52)	1.530 (8)
		C(61)–C(62)	1.530 (8)
C(6)–C(1)–C(2)	120.8 (4)	C(3)–C(4)–C(5)	121.4 (4)
C(11)–C(1)–C(2)	120.0 (4)	C(41)–C(4)–C(5)	119.1 (4)
C(11)–C(1)–C(6)	119.1 (4)	C(41)–C(4)–C(3)	119.4 (4)
C(1)–C(11)–C(12)	119.6 (4)	C(4)–C(41)–C(42)	112.0 (4)
C(1)–C(11)–O(1)	117.9 (5)	C(4)–C(5)–C(6)	118.9 (4)
O(1)–C(11)–C(12)	122.5 (5)	C(51)–C(5)–C(6)	120.1 (4)
C(1)–C(2)–C(3)	120.2 (4)	C(51)–C(5)–C(4)	121.0 (4)
C(21)–C(2)–C(3)	121.0 (4)	C(5)–C(51)–C(52)	116.4 (4)
C(21)–C(2)–C(1)	118.8 (4)	C(5)–C(6)–C(1)	119.6 (4)
C(2)–C(21)–C(22)	111.2 (4)	C(61)–C(6)–C(1)	119.3 (4)
C(2)–C(3)–C(4)	119.0 (4)	C(61)–C(6)–C(5)	121.1 (4)
C(31)–C(3)–C(4)	121.6 (4)	C(6)–C(61)–C(62)	112.1 (4)
C(31)–C(3)–C(2)	119.4 (4)		
C(3)–C(31)–C(32)	116.3 (4)		

$(C_6Et_5COCH_3)Cr(CO)_3$ (7). Pentaethylacetophenone, **6** (0.916 g, 3.5 mmol), and $Cr(CO)_6$ (3.777 g, 17.2 mmol) were heated under reflux in a mixture of 40 mL of heptane and 10 mL of THF during 3 days. Subsequent filtration and multiple recrystallizations from CH_2Cl_2/heptane gave yellow parallelpiped crystals of **7** (1.18 g, 2.97 mmol; 85%), mp 158–158.5 °C. Mass spectrum: m/z(%) 396 (1.5) $C_{21}H_{28}CrO_4$ $(M)^+$, 340 (1) $C_{19}H_{28}CrO_2$ $(M - 2CO)^+$, 312 (21) $C_{18}H_{28}CrO$ $(M - 3CO)^+$, 260 (15) $C_{18}H_{28}O$ $(PEAP)^+$, 245 (100) $C_{17}H_{25}O$ $(PEAP - CH_3)^+$, 231 (47.5) $C_{16}H_{23}O$, 217 (17.5) $C_{16}H_{25}$. IR (CH_2Cl_2): ν_{CO} 1957, 1874, 1690 (ketone) cm^{-1}. ^{1}H NMR (CD_2Cl_2): δ 2.70 (s, 3 H, $CH_3C{=}O$), 2.64 (d, ^2J = 15 Hz, q, ^3J = 7.5 Hz, 2 H, CH_2[b]), 2.60 (q, ^3J = 7.5 Hz, 2 H, CH_2[e]), 2.36 (pseudo-septet, 4 H, CH_2[c], CH_2[d]), 2.192 (d, ^2J = 15 Hz, q, ^3J = 7.5 Hz, 2 H, CH_2[a]), 1.296 (t, ^3J = 7.5 Hz, 3 H, 4-CH_3), 1.280 (t, ^3J = 7.5 Hz, 6 H, 3,5-CH_3), 1.201 (t, ^3J = 7.5 Hz, 6 H, 2,6-CH_3). ^{13}C NMR (CD_2Cl_2) at 30 °C: δ 234.47 (Cr-$(CO)_3$), 203.90 (C=O), 118.79 (C(4)), 113.88 (C(2,6)), 109.12 (C-(3,5)), 107.2 (C(1)) [the relaxation time of C(1) has a noticeable temperature dependence; the peak is rather weak at +30 °C but is sharp and well-resolved below −20 °C], 35.93 ($CH_3C{=}O$), 24.47 (2,6-CH_2), 23.30 (4-CH_2), 20.16 (3,5-CH_2), 20.00 (3,5-CH_3), 15.33 (2,6-CH_3), 14.94

(4-CH_3). Anal. Calcd for $C_{21}H_{28}CrO_4$: C, 63.62; H, 7.12. Found: C, 63.05; H, 7.32.

X-ray Crystallography. Crystals of $(C_6Et_5COCH_3)Cr(CO)_3$ were grown from CH_2Cl_2/heptane. The density was determined by suspension in an aqueous solution of $ZnCl_2$. Clear yellow parallelepiped crystals were examined under a polarizing microscope for homogeneity. A well-formed crystal, 0.55 × 0.45 × 0.16 mm, was selected and sealed in a Lindemann capillary. Unit cell parameters were obtained from a least-squares fit of χ, ϕ, and 2θ for 15 reflections in the range $20.8° < 2\theta < 26.1°$ recorded on a Nicolet P3 diffractometer with use of graphite monochromated Mo Kα radiation (λ = 0.71069 Å at 22 °C). Intensity data were also recorded on a Nicolet P3 diffractometer with a coupled θ(crystal)-2θ(counter) scan, for 3003 reflections in the hemisphere (h,$\pm k$,$\pm l$) with $2\theta \leq 45°$. The methods of selection of scan rates and initial data treatment have been described.[16,17] Corrections for Lorentz-polarization effects and absorption (ψ scans)[18] were applied to all reflections. Two standard reflections (5,-1,-2, 1.59%; and 2,-5,-2, 1.69%) monitored every 48 reflections showed no sign of crystal decomposition or instrument instability. Symmetry-equivalent data (330) were then averaged (R_{int} = 0.0076) to give 2673 unique reflections. A summary of crystal data is given in Table II.

Solution of the Structure. The coordinates of the chromium atom were found from a three-dimensional Patterson synthesis with use of the program SHELX-76.[19] Full-matrix least-squares refinements followed by a three-dimensional electron density synthesis revealed all the non-hydrogen atoms. After refinement, the temperature factors of the non-hydrogen atoms, which were previously isotropic, were made anisotropic, and further cycles of refinement revealed the positional parameters for most of the hydrogen atoms. These were included in subsequent cycles of refinement along with the remaining hydrogen atoms fixed in their calculated positions, (U fixed at 0.08 Å^2). Further refinement using full-matrix least squares minimizing $\sum w(|F_o| - |F_c|)^2$ was terminated when the maximum shift/error reached 0.057. Final R_1 = 0.0501, R_2 = 0.0547 for 2198 reflections for which $I > 2.5\sigma(I)$. Correction for secondary extinction was not necessary. Throughout the refinement, scattering curves were taken from ref 20, and anomalous dispersion corrections from ref 21 were applied to the curve for chromium. All calculations were performed on a VAX 8650 computer. Programs used were as follows: XTAL,[22] data reduction; TAPER,[18] absorption correction; SHELX-76,[19] structure solution and refinement; MOLGEOM,[23] molecular geometry; and SNOOPI,[24] diagrams. Final atomic positional parameters are given in Table III, selected bond lengths and bond angles are given in Table IV.

Acknowledgment. We thank the donors of the Petroleum Research Fund, administered by the American Chemical Society, for partial support of this research. Financial support from the Natural Sciences and Engineering Research Council of Canada is gratefully acknowledged. B.M. thanks the Ontario Provincial Government for an International Students Scholarship. Mass spectra were obtained courtesy of Dr. Richard W. Smith of the McMaster Regional Centre for Mass Spectrometry.

Registry No. 6, 77922-78-2; **7**, 123674-42-0; $Cr(CO)_6$, 13007-92-6; hexaethylbenzene, 604-88-6.

Supplementary Material Available: Tables SI-SIV listing full crystal data, least-squares mean planes and dihedral/torsional angles, hydrogen atom positional parameters, and anisotropic temperature factors, respectively (7 pages); Table SV listing observed and calculated structure factors (5 pages). Ordering information is given on any current masthead page.

(16) Lippert, B.; Lock, C. J. L.; Rosenberg, B.; Zvagulis, M. *Inorg. Chem.* **1977**, *16*, 1525.
(17) Hughes, R. P.; Krishnamachari, N.; Lock, C. J. L.; Powell, J.; Turner, C. T. *Inorg. Chem.* **1977**, *16*, 314.
(18) Calabrese, J. C.; Burnett, R. M. TAPER locally modified by Z. Tun, with the permission of the Nicolet XRD Corp., 1980.
(19) Sheldrick, G. M. SHELX-76, Program for Crystal Structure Determination, University of Cambridge, England, 1976.
(20) Cromer, D. T.; Mann, J. B. *Acta Crystallogr.* **1968**, *A24*, 231.
(21) Cromer, D. T.; Liberman, D. *J. Chem. Phys.* **1970**, *53*, 1891.
(22) Stewart, J. M.; Hall, S. R. The XTAL System of Crystallographic Programs. Technical Report TR-1364, 1983; University of Maryland: College Park.
(23) Stephens, J. MOLGEOM adapted from CUDLS, McMaster University, Canada, 1973.
(24) Davies, K. CHEMGRAF suite: SNOOPI, Chemical Design Ltd. Oxford, England, 1983.

High-Temperature ^{29}Si NMR Investigation of Solid and Molten Silicates

I. Farnan* and J. F. Stebbins

Contribution from the Department of Geology, Stanford University, Stanford, California 94305. *Received May 11, 1989*

Abstract: High-temperature (up to 1250 °C) ^{29}Si NMR T_1 and line-shape measurements were made on silicate samples with varying SiO_2 contents. The samples represented a range of bridging and nonbridging oxygen distributions from Q^4 in albite ($NaAlSi_3O_8$) to Q^2 and Q^0 in a mixture of lithium orthosilicate and metasilicate (Li_4SiO_4/Li_2SiO_3). T_1 relaxation data as a function of temperature for glassy samples showed a dramatic increase in efficiency at the glass transition. This was ascribed to relaxation by paramagnetic impurities becoming more efficient as silicon atoms and impurity ions begin to diffuse through the material at temperatures above T_g. In each sample chemical exchange was observed at high temperature, indicating that the lifetime of a silicate tetrahedron in the melt is short on the NMR time scale, i.e., a few microseconds. Variable-temperature line-shape data for potassium tetrasilicate ($K_2Si_4O_9$) allowed the exchange process to be modelled and spectra to be simulated, yielding an activation energy for the process. This was in good agreement with the activation energy for viscous flow derived from viscosity measurements. It appears that ^{29}Si NMR is coming close to detecting the fundamental step in viscous flow in silicates with good agreement between the time constant of the exchange process determined by NMR and the shear relaxation time of the potassium tetrasilicate liquid.

Understanding of the physical chemistry of silicate liquids is important in both the earth sciences and material science: the chemical and physical behavior of magmas dominates many geological processes, and most technological glasses and glass ceramics start off in the molten state. Our present knowledge of these systems is limited, however, by the technical difficulties of working at high temperatures, and the theoretical complexities of materials whose structure and dynamics lie somewhere between the relatively well-understood field of organic polymers and that of molten salts.

0002-7863/90/1512-32$02.50/0